GIS Atmospheric Chemical Fate Model Simulation of Iron Released from High Intensity Bombing in Northwestern Laos

U. Gonzalez[1][*], D. Patton[2], and G. W. Huang[3]

[1] *Model-set Research and Development, 79250 Cool Reflection, La Quinta, California 92253, USA*
[2] *School of Information and Physical Sciences, University of Newcastle, New South Wales 2308, Australia*
[3] *Graduate School of Global Environmental Studies, Sophia University, Tokyo 102-8554, Japan*

ABSTRACT. The atmospheric dispersal of iron fragments ejected from detonated ordnance released within the Nam Souy sub-basin during the secret bombing campaign of Laos from 1965 ~ 1973 was simulated through python integration with ArcGIS. The data for the study was obtained from the US National Archives and shows that of a total of 7,667,619 weapons delivered in Laos (4.5 million tons), 19,005 (5,900 tons) were dropped within the study site. The simulation adapted Gaussian isotropic puff modeling for the dust/grain-sized fragments and explosive force radial release modeling for the larger fragments into python script to produce temporal raster output images of the dispersal patterns of the analyte. The use of code language libraries ArcPy, NumPy, and numba and the logic for their application is discussed and reported along with the script developed. The simulation produced 9 m^2 resolution raster images displaying iron material loading at ground level. Loading density is reported at a range between 0 ~ 7.5 g/m^2 washable iron load, 0 ~ 0.65 kg/m^2 of suspended iron load, and 0 ~ 3.5 kg/m^2 of bedded load. The results are intended for use in subsequent studies of surface removal over time with a potential application in exposure risk analysis and for the assessment of impact on natural environments.

Keywords: atmospheric material dispersal, chemical fate modeling, environmental risk assessment, Geographical Information Systems, high intensity warfare, iron, ordnance, Python

1. Introduction

As humanity witnesses continuous high-intensity warfare and ten-year wars becoming more commonplace, extremely large quantities of ordnance are frequently scattered throughout the world (WIIPA, 2016). Considering the continuing trend and the high possibility of more large-scale bombing campaigns occurring in the near future, it is necessary to understand the implications of these activities on environments and particularly within human habitats. Surely the killing of innocents and the destruction of communities by bombing activities is tragic and upsetting, it is also crucial to consider the post war impact of largescale bombing; to quantify and track the fate of all the substances introduced into the environment experiencing war. Because of the excessive amount of material imported into the sites experiencing high-intensity combat, it is important to understand the dynamics and consequences of the deposited material, which in many cases amounts to millions of tons of a contaminant that may have health implications for generations.

According to mass balance/mass transfer principles, the dispersal of chemical pollutants throughout an environment can be reliably modeled, measured, and tracked, exposing the risks on the environment and on human health (Suter II, 2016). Thus, after impact, detonation, and dispersal, the various chemical components that constitute ordnance can be tracked though modelling and subsequently validated though chemical analysis. A model – or set of models – which can be used to determine the movement, fate, and abundance of the materials disseminated from detonating ordnance can then provide greater insight into the behavior of these materials within an environment and subsequently uncover potential ramifications.

During the years of the war between the United States and the North Vietnamese Communist Party – known as the Vietnam War to Americans – the United States Central Investigation Agency (CIA), with the assistance mainly from the United States Air Force (USAF) but also from other military commands, conducted a secret bombing campaign in the Peoples Republic of Lao (McCoy, 2002). From 1965 to 1973, the United States military dropped approximately 4.5 million tons of ordnance throughout Laos – therefore, making it the most densely bombed country in the history of warfare (Khamvongsa and Russell, 2009). This unfortunate reality makes Laos the ideal candidate for developing and testing the detonated ordnance mass balance and chemical fate model-set to understand the potential dispersal patterns of these materials throughout the environment.

* Corresponding author. Tel.: +1-442-899-8893.
E-mail address: gonzalezu01@gmail.com (U. Gonzalez).

This project intends to contribute to the development of a comprehensive mass balance model-set for determining the dispersal, endpoints and concentrations of the iron derived from detonated bombs. Considering that iron represents roughly half of the weight of most ordnance deployed during the aforementioned bombing campaign (Department of the Army Technical Manual, 1966), it was considered a valuable starting point to test a mass balance/fate model-set. Such a model could potentially be referenced for any largescale ordnance detonation event; this model application uses the bombing campaigns in Laos as a case study.

Through the model, it should be possible to find the major sinks or endpoints of the iron released from detonating ordnance for the intended study site. It is developed based on the characteristics of the bombing campaigns conducted in Laos and related to the specific amount of material input of iron in a specific area of the country along with the physical-chemical characteristics of this site. Fortunately, the United States National Archives contain a fairly complete record of the bombing campaigns conducted in Laos during these years. With coordinates, bomb types, and bomb quantities, it is possible to create a very descriptive material input inventory that will be essential for the applicability of the model.

With the help of GIS software, it is possible to observe a simulation of the dispersal patterns of the material released from detonated ordnance. By applying a well-developed model-set and integrating this into GIS software, given reliable parameters, sites of material concentration and estimates of fugitive material can be obtained. In this study a python script was written using the ArcGIS supplemental tool ArcPy with which data was accessed, processed, and applied to the model, producing a simulation of material dispersal. Temporal maps generated can allow for an analysis of influx and outflow from the system over time.

The site chosen is one that is considerably safe to navigate within and that has experienced a considerably high amount of ordnance material input; for the sake of obtaining valuable evidence. Thus, for the Nam Souy sub-basin of the Nam Ngum River Basin on the western side of Xiangkhouang Province of Northeast Laos (Figure 1), a full inventory of input iron was created for ordnance dropped within this area, and a subsequent fate model was developed based on the nature of the chemical components, the characteristics of the soil, weather trends, topography, bodies of water, and surface runoff; these qualities or variables being influencers in the dispersal or sequestration of the contaminants.

In order to develop a model-set to observe material dispersal, it was thought necessary to divide the dispersal into phases within which models can reliably evaluate material endpoints at medium boundaries. The first phase of material dispersal includes the dynamics for material that is thrown into the air as ordnance detonates. From this phase, as the material reaches the ground new forces and processes influence its fate. Thus, a model-set for atmospheric dispersal and another for surface dynamics were developed. This report solely considers the dynamics that influence the movement of detonated ordnance released iron into the atmosphere. The second report will be subsequently presented.

To develop a reliable model-set for atmospheric distribution of the released material, a combination of an explosive radial release model used for the fraction of larger fragments unsusceptible to atmospheric turbulent forces and an isotropic gaussian puff equation for the fraction of smaller fragments that are susceptible to turbulent transport were employed. The former is an adaptation of Boughton and DeLaurentis (1992) explosion radius equation used to determine explosion cloud top height and radius. The later is a modification and integration of Pistocchi's isotropic gaussian plume equation with Zannetti's non-reflective gaussian puff equation (Zannetti, 1986; Pistocchi, 2014). The fragment sizes where parameterized based on results from Cohen's simulation of the Mott equation for predicting exploded warhead fragment weight distribution (Cohen, 1981).

Pistocchi (2014) presented a rather complete methodology for simulating a gaussian distribution for assessing chemical fate by using the tools available in the ArcGIS toolset. Considering the nature of the contamination events considered for this study, the applicability of this methodology was limited. While the tools and methods described by Pistocchi were valuable for designing this report, the Isotropic Gaussian Plume model employed by him was not applicable and neither was the Arc-GIS tool-set capable of managing the nature of the dataset used for this study. The study required a model descriptive of discrete puff emissions for thousands of data values as well as the need to apply Python code to process the large amount of data through the model.

To test the reliability of the model-set, a chemical analysis of the site should be conducted, as noted by Suter II (2016); nevertheless, this analysis does not pertain to the scope of this study which is a remote simulative study based on the available resources found on the internet and within literature as well as computer tools to help explain the implicated processes of material dispersal and fate. The results provide valuable evidence of an altered chemistry within the soil, sediment, and water bodies. In the case of materials with toxicological significance, the observations of the distribution of these chemicals are believed to provide indispensable data for evaluating exposure risk and for conducting human health risk assessments.

2. Project Design

2.1. Study Site

The site chosen is the watershed of to the Nam Souy sub-basin which sits in the Nam Ngum River Basin. It is in the northeastern part of Laos on the west side of the Xiangkhouang Province. The village of Muang Souy lies at the heart of the watershed and the stream outflow is located at 19°30′34″N, 103°02′55″E (Figure 1). The watershed measures approximately 242.57 square kilometers. Based on the digital elevation map obtained from the Japan Aerospace Exploration Agency's map databank (2020), the upstream of the watershed is rather hilly but flattens out as it reaches the Nam Ngum River. The Nam

Ngum River runs southwest and feeds the Nam Ngum Reservoir which provides power and water to the capital Vientiane and the surrounding villages (Jayasekera and Kaluarachchi, 2015). The outflow stream of this dam is a tributary to the Mekong River. The town of Muang Souy does not have any large-scale development; the farming at the lower altitudes is also of very modest intensity as can be seen by the most recent aerial images provided by Google Earth (2023).

Figure 1. Map of the study site (the village of Muang Souy at the heart of the watershed; the Nam Souy outlet at the junction of the Nam Souy River with the Nam Ngum River).

2.2. Agent Characterization

The two main iron-based materials to be parameterized are steel and various other, mostly unspecified, iron materials. While iron materials and steels have varying chemical fractions based on purpose and manufacturer, and the weapons inventory as well as military manuals are not particularly clear about the component steel types, it is considerably difficult to calculate a precise iron fraction for all of the inventory weapons included in the modeling. Based on studies reporting warhead casing fracturing performed by Goto et al. (2008), Stronge et al. (1989), Cohen (1981), the iron fractions of the materials tested are approximately: 99% Fe (AISI 1018 steel), 99% Fe (Armco iron), 99% in low carbon steel, respectively (Watmough and O'shea, 1977).

By combining the iron fraction estimate within the iron materials along with the proportion of missile/rocket components which are assumed to be composed of iron and steel, the parametric value for iron content of the total weapon weight is approximated at 41% of the total bomb weight. These iron parts include the weapon body, the warhead casing, and the main fins. The rest consisting of the nitrogen-based explosive, aluminum jacket/fins, some electronic accessories made of plastic, conducting metals, etc. This is a broad simplification of the parameter considering the variety of weapons used and the varying reference values. Nevertheless, it represents a low estimate; true iron content values are expected to be closer to 50% of the bomb weight (Department of the Army Technical Manual, 1966).

Two main properties of iron influence the containment and subsequent release of the explosive: ductility and the ability to fracture. By default, a metal casing is used for ordnance because of its durability and structural integrity. And over the years, it has been unnecessary to change the materials for stronger materials because it would sacrifice the ability to expand and subsequently fracture accordingly. As Stronge et al. (1989) made notes, the correlation between fragmentation and ductility is integral for proper expansion and explosive release. While the release of iron from a warhead is well documented, the fracturing and distribution of other iron materials is not so clear.

Discussed to greater detail in the next section, iron fracturing due to explosive expansion produces fragments of various sizes. The smaller sized fragments and partial surfaces of larger fragment sizes mixed with the explosive energy of detonation produce excessive heating and possible chemical modification. Potential oxidation and aerosol behavior may be a result of these fragments of "pyrogenic nature", characteristics that potentially increase iron solubility (Ito, 2013).

2.3. Modeling Atmospheric Dispersal

2.3.1. Parameter Considerations

The actual predictability of the dispersal of these materials is rather complex considering the different phases in affect, and the variables/parameters involved. Explained with detail in the next section, the adopted model for describing the distribution of materials released from detonations is composed of two basic descriptive patterns of distribution. The first pattern relates to the explosion radius to describe the radial spread of detonating ordnance material as a result of the explosive energy pushing out in this radial manner. The second pattern involves the atmospheric/environmental forces which then intervene. To apply these descriptive patterns to a modeling simulation of materials from exploding ordnance requires another step which describes the nature of the materials as they are released.

Although Boughton and DeLaurentis (1992) describe the distribution of explosive material in an environment in which they distinguish between the two phases, explosive force (puff velocities) and atmospheric (Gaussian) turbulent patterns, the study is concerned with predicting radiological fallout from a nuclear weapon; it can only partially describe the result from a conventional weapon and especially concerning the non-explosive content of the ordnance concerned. Cohen's studies detail the fracturing processes suffered by the casing of a weapon, occurring somewhere within the threshold of the ignition phase and the blast phase (Cohen, 1981). Using the Mott model, Cohen describes how the fracturing of an explosive casing produces a predictable number of fragments of predictable fragment size distribution. Based on the size distribution of casing fragments, it becomes obvious that much, if not most of the fragments cannot be greatly influenced by atmospheric dispersal processes. These larger fragments would surely only move in a projectile fashion.

Aside from the fragments experiencing a somewhat projectile behavior, only the smaller sized fragments would then be available for meaningful dispersal by atmospheric forces. By

using Cohen's simulation of the Mott equation, it is possible to obtain a value which can be used to represent a more realistic fraction of iron fragments which would be subjected to atmospheric dispersal forces and those fragments that would not suffer much influence from atmospheric forces (Cohen, 1981). Based on the results of Cohen's experiments, we obtain the weight distribution of the fragments. The fragments reported as less than one grain (0.0648 g) were too small to count but represented approximately 0.9% of the total fragment weight (Table S1). It may seem like a negligible amount, yet concerning the vast amount of total iron input, this value still represents a significant total amount of material available for dispersal by atmospheric forces.

As for fragments greater than 1 grain in size, these can be assumed to be invulnerable to diffusive dispersal patterns in the atmosphere. Considering the size range for this fraction of iron – suspended and bedded fractions from Table S1 – this study will assume that its dispersal in the atmosphere is only dependent on the force of the blast and the parameterization related to this event.

2.3.2. Projectile Dispersal Patterns

Abdul-Karim et al. (2014) mention a possible material distribution directly proportional to explosive weight, $r = w^{1/3}$. This is only an assumption on trend and relates to Church's equations on cloud top height and radius (Church, 1969). Describing it in greater detail, Boughton and DeLaurentis (1992) propose a model based on Church's initial schematic. In complete form, their model parameterizes gravitational force g, the specific heat capacity of air c_p, air density ρ, absolute temperature T, adiabatic lapse rate Γ, energy released ζ, average temperature gradient in the troposphere $\delta T/\delta z$, the entrainment coefficient α, and "functions of functions of scaled time" ξ. The equation, as the author notes, is absent of frictional drag, which would produce a shorter distance in real situations. The general equation for explosion radius which represents the reach of the fireball rather than the blast takes the following form (Boughton and DeLaurentis, 1992):

$$R_j(\zeta) = \left(\frac{3}{\pi}\right)^{\frac{1}{4}} (ak)^{\frac{1}{4}} \left(\frac{g\zeta j}{c_p \rho T}\right)^{\frac{1}{4}} \left[\frac{g}{T}\left(\frac{\delta T}{\delta z} + \Gamma\right)\right]^{\frac{1}{4}} \xi \quad (1)$$

with parameters input, the equation relates explosion radius to explosive mass, where:

$$R_e = 19.5 w^{\frac{1}{4}} \quad (2)$$

This is a modified formula from Boughton and DeLaurentis, where w is calculated in kilograms as opposed to pounds. This equation produces realistic distances within which we can expect a consistent settling of large fragments in equal distribution. Abdul-Karim and colleagues demonstrate a settling pattern where a group of fragments of larger cumulative mass is more densely settled further from the epicenter (Abdul-Karim, 2014);

but also, they mention of possible distribution of fragments following the inverse square of the radius; for this study, it will be assumed that the distribution within the explosion radius is equal throughout the ground surface area.

2.3.3. Gaussian Puff Distribution

The Gaussian plume equation is not adequate to describe the spread of emissions from a detonated weapon device. For an instantaneous release of a known mass, it is necessary for the gaussian distribution to emulate a discrete event – and applicable to multiple discrete instances – of set mass loading. Additionally, the modified gaussian must also consider that for a non-gas the floor surface will not reflect the substance. For this, Zannetti (1986) proposed the gaussian puff equation under no assumption of a reflective surface. The Equation (3) describes a mass M, loaded at puff center $p = (x_p, y_p, z_r)$, giving a concentration at receptor point r (Zannetti, 1986):

$$C(x_r, y_r, z_r) = \frac{10^9 M}{(2\pi)^{3/2} \sigma_h \sigma_z} \exp\left[-\left(\frac{x_p - x_r}{2\sigma_h}\right)^2\right]$$
$$\cdot \exp\left[-\left(\frac{y_p - y_r}{2\sigma_h}\right)^2\right] \exp\left[-\left(\frac{z_p - z_r}{2\sigma_z}\right)^2\right] \quad (3)$$

where concentration C is obtained in μg/m³, hence the factor of 10^9; the h subscript under the gaussian variance coefficients σ represents a dispersal variance applicable to both the wind direction x, and the crosswind direction y on the horizontal plane.

2.3.4. Isotropic Puff Standardization

Because there is no meteorological data collected during the period of the air raids (JICA and MOAF, 2001), wind velocity and wind direction are unknown. For this situation, Pistocchi provides a very convenient adaptation of the gaussian model to a condition which does not need to regard for wind direction. The isotropic gaussian distribution pattern, as its name indicates, describes the radial distribution of material from a source in the absence of a clear wind direction parameter, be that for instances of constantly changing wind patterns, or when no information is available. The equation produces a concentration as a function of radial distance r, in the following fashion (Pistocchi, 2014):

$$C(r) = \frac{Q}{2\pi r \sqrt{D_y D_z}} \exp\left[-\left(\frac{v}{4rD_z}\right)\right] \quad (4)$$

where r is the radial distance from the source in all directions, Q is the emissions rate, and the windspeed v replaces the vector u. It is important to note that Equation (4) is also a plume equation and assumes steady-state conditions. Furthermore, the equation seems to be adapted from an already simplified equation which analyzes concentration at ground level.

In order to apply an isotropic distribution to the data of

exploding ordnance which does not parameterize wind direction, it needs to be adapted for discrete emission events and for assessing the input at ground level, the equation should solve for mass flux onto the ground surface. Thus, we obtain an isotropic puff equation by combining Equations (3) and (4):

$$Q(r) \; = \; \frac{M}{2\pi r \sqrt{D_y D_z}} \exp\left[-\left(\frac{r}{2D_y} \right) \right] \exp\left[-\left(\frac{vz_p}{4rD_z} \right) \right] \qquad (5)$$

where Q now represents mass flux to the ground surface in kg/unit area and z_p is the puff center, when the equation solves for ground level. Here, more assumptions become evident; there are no obstacles being considered, and the surface is assumed to be flat, as Zanettii (1986) made clear as well. This equation is valuable, not only for instances when meteorological data is unavailable, such as for this study, but especially because this model is intended for risk, or predictive, studies of chemical fate.

3. Tools and Methodology

3.1. Data Retrieval and Processing

Weapons Inventory Database: The preliminary data of all the ordnance dropped within Laos was obtained from the United States National Archives (Department of Defense, Joint Chiefs of Staff, 6/1/1965 ~ 10/31/1973). The data describes the quantity of ordnance dropped, the name of each type, the coordinates where they were released, the date of release, and other attributes. The data is not organized on a per weapon basis, but rather, for every bombing sortie mission executed. The data was processed, organized, and converted into csv. format. The data exclusively from the Laos bombing campaigns were isolated for further processing. The data was accessed and filtered through python script coded on Visual Studio Code. Here the unneeded attributes of the data as well as faulty data was filtered out and only data attributes valuable to the study were kept. Finally, the data was filtered by the same means for data relevant to the study site.

3.2. Model Design and GIS Familiarization

3.2.1. Geographical Datasets

The maps and datasets obtained were accessed from the Japan Aerospace Exploration Agency (JAXA) and the "Open Development: Laos project". JAXA has the ALOS Global Digital Surface model containing 30×30 m resolution digital elevation maps for the study region available for free through registration. This resolution becomes the reference which was adapted to all of the map functions, processes, and outputs for consistency and universal applicability in all processes. These map sets were downloaded and projected from a Geographical Coordinate System (GCS) to a Projected Coordinate System (PCS) using the Project Raster tool of ArcGIS (ESRI, 2019). From Open Development: Laos, administrative maps of Laos and its provinces were obtained for general area reference (Open Development Initiative, 2023).

3.2.2. Watershed Delimitation

The program used for this processing was ArcGIS: ArcMap version 10.6. The DEM was processed to obtain a flow accumulation map and identify the outlet point. The entire upstream surface contributing flow to that point represents the watershed surface which was obtained using the Watershed-Hydrology tool of ArcMap. The result was a polygon map feature delimiting the watershed – the limits of the study site – which then was used to clip all the prior maps mentioned and the maps created from the modeling output results.

3.3. Weapons Data-Import and Python/ArcPy Processing

The weapons inventory data file was accessed by code. It was filtered for relevant data and attributes while null values and erroneous inputs were removed as illustrated in Figure S1, "ThorProc.py". The exclusion criteria for the data can be observed here. Next, using the watershed delimitation map borders, the data is clipped using ArcGIS Pro *Raster Clip* tool, which produces a new data file containing the datapoints that belong to the area of interest (ESRI, 2020). The complete code for each stage, and other resources created or accessed for this project can be accessed at: https://github.com/Superguy2876 /Gauss-Iron.

For purposes of temporal analysis, the data was read on a yearly basis, the year starting from the start of the bombing campaign within the study site and ending 365 days later (Figure S2). This report does not perform any perform any particular analysis of temporal mass balance, yet this is done for the next phase of the study, temporal analysis for surface removal of iron.

3.3.1. NumPy Array Processing

The Python NumPy library, which is a set of mathematical tools for python, was used to process the map data in array pattern with the tool, NumPy Array. In this manner, data distributed in a grid layout such as on a raster map could be processed in place – according to location reference attributes of the data, using the numerical function operators available within the language. The NumPy Array tool allowed for the data to be processed through the function and for the results to be redisplayed on a new output raster using the ArcPy language library tool 'NumPyArrayToRaster' as can be seen in Figure S3.

3.3.2. Numba Processing

The numba jit compiler was used to more efficiently process the NumPy code. This allows for the reduction in processing time as well allowing for efficient use of full hardware capacity to perform the processing. As can be observed in Figures S4 and S5, Numba was applied to the code at two vital points: for compiling the code into machine code for faster processing and processing the array in parallel.

3.4. Python Processing of Atmospheric Models

3.4.1. Model Function Parameter Application

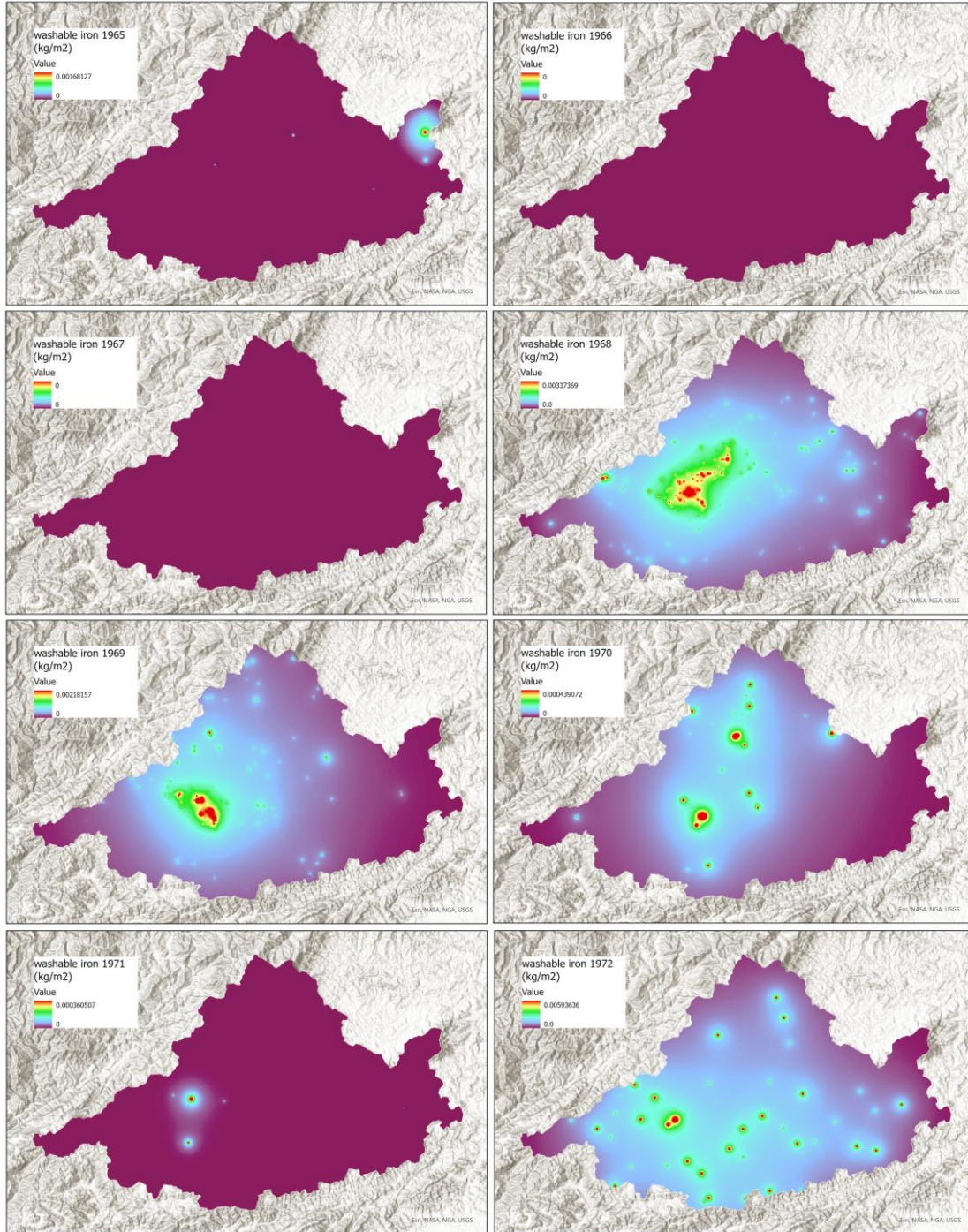Figure S6 shows the set parameters accessed throughout

Figure 2. Temporal output of the Gaussian Processor (washable iron) simulated on ArcGIS Pro (1965 ~ 1972).

the script and simply apply the necessary modification to the original data values present in the dataset.

3.4.2. Gaussian Atmospheric Distribution GIS Simulation

The material defined within the "washload" fraction of iron fragmentation was processed using the isotropic gaussian puff Equation (5) and was adapted into the ArcPy script func-

tion as can be seen in Figure S7. With the help of NumPy Array, the function was processed more effectively, and efficiency was facilitated by parallel processing from the numba compiler. The data was processed through the script and projected as a raster using the ArcPy 'NumPyArrayToRaster' tool. This was done for the data pertaining to every year interval defined in Figure S2 and produced temporal raster outputs of washload iron influx at the study site.

3.4.3. Explosion Radius Distribution GIS Simulation

In a similar manner as with the washload atmospheric distribution, the explosion radius function was applied to the fractions pertaining to the remaining fragments which were not evaluated as being susceptible to atmospheric turbulence. The explosion radius Equation (2) was adapted into the code (Figure S8) as 'staticProcessor'. The function was processed through a NumPy Array as with gaussian atmospheric distribution. The processing output results were rasterized with the 'NumPyArrayToRaster' tool. The rasters produced represent each year interval defined, as with the washload atmospheric distribution.

4. Results and Discussion

Of the total sorties carried out within Laos, 407,299 were from the usable data and 1,181 of these sorties were conducted within the site. The former sorties account for 7,667,619 weapons delivered, while the study site received 19,005; these represent 4.5 billion and 5.9 million kg, respectively, of iron material released in the country and the study site. It is not necessary to perform fate modeling to conclude that the excessive input of iron is astonishing and of significant environmental concern. The mass balance model serves to make evident the extent of contamination. The fate model on the other hand, becomes valuable for pinpointing the sinks and degree of iron concentration at different locations within the study site. These identified locations serve as points of interest for future studies. The GIS simulation contributes even more so by allowing for the visualization, first, of the scale at which this area was utterly destroyed through massive bombing campaigns, but in more detail, of the distribution of the dispersed iron materials throughout the area.

4.1. Isotropic Gaussian Puff Simulation

As can be appreciated from Figure 2, the Isotropic Gaussian puff simulation produces radial dispersal from the group of discrete point sources representing impact sights. Although in some locations, larger ordnance produces more material dispersal due to the amount of material released – not related to the explosive content – some of the more densely colored points actually represent sites where multiple weapons were released at or near to prior ordnance release points (Figure 3). While years 1966 and 1967 don't seem to have any material intake, and other years have few events and some show significant activity, Figure 3 shows the totality of the events that occurred in the study sight.

The loading range for the cells conforming the study site falls between 0 and 177 g of iron within cells of 9 m^2. We see a maximum loading at about 7.5 g/m^2. This may not seem to be significant, but roughly 21,439 kg of washable load are distributed throughout the entirety of the study area (approximately 250 km^2), which is only a fraction (0.89%) of the actual total iron dispersed throughout the study site and represents a considerable change in small fragment loading into the site.

A 3 × 3 resolution raster cell may seem like a baseless resolution choice, yet it was chosen to obtain a more precise simu-

lation for further use while sticking to a multiple of 30 × 30, at which the highest available digital elevation map resolution for the study site is set at, with which subsequent surface flow/removal analyses can be conducted. This chosen resolution is also the highest and most practical resolution obtained, based on our criteria of need, functionality, and cost benefit. The same 8 maps weigh close to 50 Gb of data at 1 m^2 resolution and take a couple days to process and output, while the ones reported here represent close to 5 Gb of data and take 2 or 3 hours only. Thus, if applied to a greater area, the process would overwhelm the processing and memory capacity of the systems used.
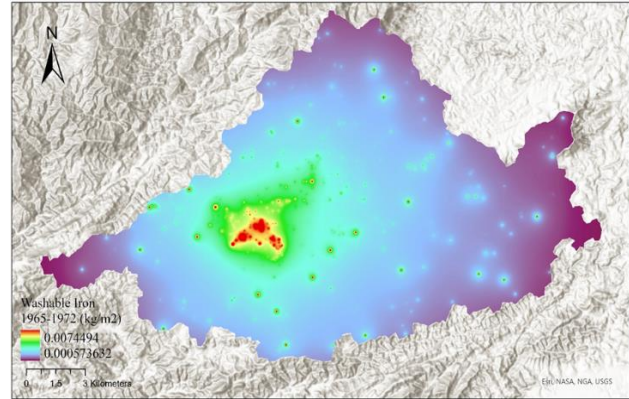

Figure 3. Full washable iron loading of Nam Souy sub-basin from 1965 ~ 1973.
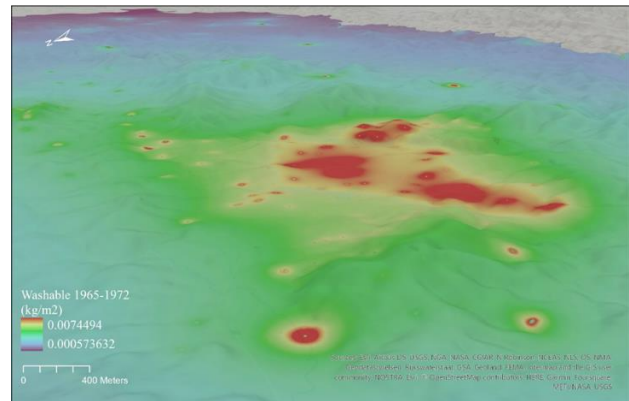

Figure 4. Birds-eye view of the watershed from the northwest.

Another limitation to be noted is the fact that the gaussian puff equation considers a puff center height with relation to a ground with no contour. In a real environment, the value of ground level with respect to the initial puff center is variable. With some time and effort, the script can be adjusted so that the model takes into account surrounding surface contour. While the hill shaded map of Figure 4 shows the material applied onto a three-dimensional contour, this is misleading considering that the contour would block some material flow in the air and there would potentially be shadows of material. Nevertheless, the significance of this may be small compared to the uncertainties produced by the other parameter limitations. More studies are necessary to support this claim.

4.2. Explosive Radius Simulation

As can be seen from Figures 5 and 6, the distributions of iron as a result of the explosion radius distribution simulations seem rather limited compared to the distribution patterns shown in Figure 3, to the extent that the distribution of loading in Figure 5 isn't impressive visually. This observation is misleading, though, due to the fact that the scale for Figure 5 is significantly greater than that of Figure 3. This means that the reach of material dispersed by atmospheric turbulent forces is greater even though the distribution peak of Gaussian loading (Figure 3) is appreciably low compared to the other two loading fractions which contain significantly greater loads of iron (Figure 5). The loading of the washed fraction to the ground surface adds little to cells where suspended and bedded loading occurred. The range of suspended iron loading is roughly from 0 ~ 0.3 kg per cell, a maximum loading equivalent to 0.065 kg/m^2, over around 10 times greater than the maximum washable loading. The distribution of the maps from Figures 5 and 6 are identical because of the fact that the explosion reaches, and material load proportions are identical as per Equation (2). Nevertheless, the scales are different by 5000%, which is rather significant. It is also important to note that the processes which follow material settling from the atmosphere influence this initial distribution differently and the fate simulations would differ for each load fraction. Finally, if all three atmospheric distribution maps were put on the same scale, the display intensities would differ greatly.

5. Conclusions

5.1. Watershed Delimitation

The implementation of the Watershed tool available in ArcGIS version 10.6 allowed for the appropriate identification of a study site based on topographic elevation, flow direction, flow accumulation, and watershed outlet as parameters. The resulting watershed map was appropriately georeferenced, of higher resolution, and dependent of the actual ridges which delimit and isolate surface which induces flow towards separate watersheds, as compared to any watershed map found in literature. This procedure is considered valuable for any future watershed study for any purpose but specifically for fate modeling, and exposure analysis.

Chemical fate analysis is shown to be more effectively analyzed by using watershed limits to delimit a study site, as opposed to political boundaries, or other arbitrary boundaries that are not physical limits which influence the dispersal of materials throughout the environment. Watershed limited fate analysis will produce reliable results by pinpointing sinks and other accumulation hotspots. The effectivity of this study was strengthened by adopting this limitation strategy. Although the atmospheric transfer of material may seem less dependent on watershed limits, using watershed ridges as natural boundaries is practical for application in posterior steps of chemical fate analysis and is a necessary starting point within the scope of this report.

The watershed delimitation strategy can be faulty. If incorrect outflow points of a stream system are indicated, the tool will produce varying results which should be double checked. The strategy can be improved in terms of precision with the availability of higher resolution digital elevation maps. It was necessary to have prior knowledge of the outlet coordinates in order to identify the correct outlet point within the flow accumulation map.
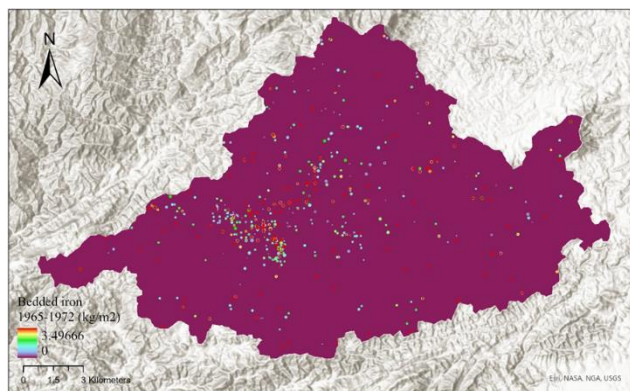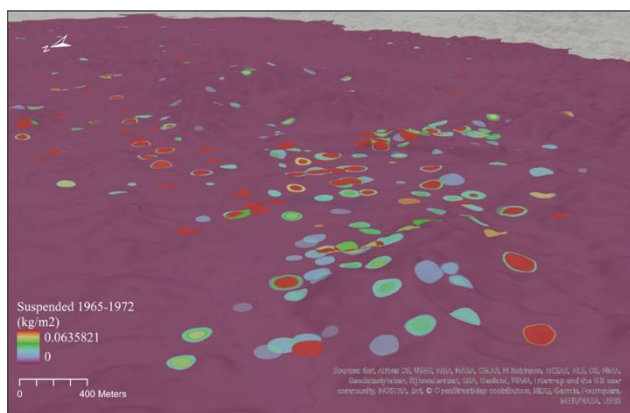

Figure 5. Distribution of the bedded load of iron.

Figure 6. Distribution of Bedded load of iron with closer 3D contour view.

5.2. Fragment Size Fractioning

By applying a fragment size distribution to the iron fragments, it was possible to consider more plausible distribution patterns throughout the environment due to different physical-chemical characteristics of these different size categories. The Mott equation and Cohen's fragment distribution results allowed for this parameterization within this study. It is considered appropriate to assemble fragment size ranges into size/weight categories which can define the processes undergone by the materials throughout an environment. By reducing assumptions throughout the model set which describe these processes and patterns, the spatial distribution of the various fractions can be more accurately traced.

Neither the modeling of the Mott equation, nor Cohen's results are sufficient for producing precise fraction values nor categories for weapons of varying constitution and conforma-

tion. Cohen's study demonstrates the different particle size distribution between two material types; thus, it can be assumed that there is significant error in applying the same fraction values to all the weapons of this study of not fully known material composition and weight distribution. The burden of fractioning parameterization should be placed on the manufacturers which should provide this data for every explosive weapon model produced along with each adaptation and variation of each weapon. An ERA for ordnance release into environments with institutional leverage and social value could potentially force manufacturers to provide such detailed information. If posterior studies are to find significant exposure risk based on the preliminary observations of this study, such legal implementation of limitations and the assigning of responsibilities is justified.

5.3. Atmospheric Modeling of Ordnance Material Transport

It is conclusive that the dynamics of explosive dispersal of ordnance materials should be combined along with environmental dispersal forces to describe the spatial distribution and fate of materials throughout an environment. Although the models adopted seem to consider the main driving forces for material release and transport, there seem to be many holes within the parameterization but also within the model structure. Surely, the results would be more accurate if the presented models were complete with parameter and variable data, nevertheless, it is also impractical to expect such parameterization for predictive modeling for which little preliminary data may exist and parameters are adopted from previous normal values and averages. Whether or not a more complex model set which considers more variables can be a more accurate descriptive tool of material distribution and fate is unknown, such comparison is not achieved from the results of this study.

Because the main parameters for these events were considered – including discrete puff events, diverse fraction distribution patterns, explosive weight and material loading dependent model terms, etc. – a general and appreciable distribution simulation gives insight into the loading potential of such events for the different environmental medium within a watershed. As for the assumptions towards the extent at which each atmospheric distribution model intercedes in the distribution patterns of the material, considering that the pixel resolution adapted to the simulation is rather limited and more so if undergoing surface removal simulations dependent on lower resolution DEMs, these are considered acceptable. In the situation where the resolution describes more detailed loading values, the sequential and overlapping extent of the various models adapted could be more specific.

The evaluation of surface flux from the atmosphere – the analysis at height = zero – was sufficient for assessing the chem- ical fate. In an exposure analysis, it may be necessary to consider atmospheric distribution at points other than ground level due to the possibility of inhalation or dermal contact by bystanders. This observation should be considered if such exposure risk exists, especially for materials of corrosive, radiological, or acute damaging potential. The greatest risk for iron

may be dust infiltration of the lungs and possible subsequent absorption; being that the general presence of civilians at these sites is unknown, the disregard of such within this study was acceptable.

The explosion radius distribution pattern adopted for evaluating surface loading seems to contain less potential error considering that the assumptions of equal spatial distribution throughout the explosion area reflect very realistic results. Due to the low permanence of these fractions in the atmosphere, an evaluation at ground level is appropriate for chemical fate analysis. Additionally, the larger fragments have less influence on immediate surface removal and transport.

5.4. Surface Removal, Accumulation, Fate, and Subsequent Steps

The model-set used for this report were developed simultaneously with a larger model set that includes parameterization, modeling, and simulation of surface removal, accumulation, and chemical fate. The present report is insufficient for assessing fate, or limited for observation at the atmospheric, soil boundary layer. Surface transport of material was simulated, and the results will be presented in a separate report. The models of both reports represent a model-set and are interdependent for the purpose of assessing chemical fate, and for any posterior analysis/uses they may serve. The analysis of surface removal should give insight into the fate of washed iron into the stream systems, and eventually into the ocean. If such can be evidenced though the validation – through chemical analysis – of the combination of the model-sets presented in this study and those employed for surface removal and fate modeling, it may be possible to determine the intensity of material loading at the ocean for iron derived from exploded ordnance released during the Vietnam War era.

The application of a chemical analysis of the site would produce valuable insight concerning the reliability of the model set. Similarly, the complete model set can help identify the locations within the study site of particular interest, being these the zones identified with the highest loading rates. These locations represent the areas of interest for post analysis of chemical fate and exposure risk. Because the washable load represents a minute fraction of the total iron input, the locations of material input marked in the bedded and suspended load maps are of particular importance considering that most of the material is focused on these sites and studying these through chemical analysis can provide validation of the models used as well as give insight towards the chemical changes undergoing at these locations.

A chemical analysis would require distinguishing from natural occurring iron species and those derived from the exploded ordnance. Thus, it is crucial for an in-depth risk assessment to identify the varying chemical species of the analyte as well as indicators of distinction between these and the natural varieties present in samples. Furthermore, for the model to be fully verifiable, the entirety of material input needs to be evaluated.

5.5. Importance of Assessments of Environmental Risk for High-Intensity Bombing and Applicability in Contemporary Events

Considering the events revolving around the conflict in Ukraine and the ongoing conflict activities in the middle east, a well developed and validated model-set is vital for determining the potential ramifications of high-intensity warfare on the environment. The tools provided from this study – complemented with tools and data derived from a study of surface removal of iron to analyze chemical fate and the validation of these through chemical analysis on the field – can be used to assess an exposure risk of high concentrations of iron distributed through an environment such as the study area. If exposure risk can be verified, then the applicability of a well-developed model-set for mass balance and chemical fate analysis will be of utmost importance and addressing the environmental risk presented by contemporary high-intensity warfare.

While this study only considers iron as the analyte, it is important to take into account that if contemporary weapons contain other chemical components of potentially high toxicological significance, then the adaptation of the model-set parameters from this study may give insight into the fate and risk of exposure produced by the implementation of such weaponry. As a result, better informed decision making can be implemented towards the application of toxic chemicals in the development of present and future tools of war.

References

Abdul-Karim, N., Blackman, C.S., Gill, P.P., Wingstedt, E.M.M. and Reif, B.A.P. (2014). Post-blast explosive residues - a review of formation and dispersion theories and experimental research. *RSC Advances*, 4(97), 54354-54371. https://doi.org/10.1039/C4RA04195J

Boughton, B.A. and DeLaurentis, J.M. (1992). *Description and Validation of ERAD: An Atmospheric Dispersion Model for High Explosive Detonations* (No. SAND-92-2069). Sandia National Labs, Albuquerque, NM (United States).

Church, H.W. (1969). *Cloud rise from high-Explosives detonations*., Sandia National Laboratories (SNL), TID-4500, 53rd edition, UC-41, (1969) 14. https://doi.org/10.2172/4798257

Cohen, E.A. (1981). New formulas for predicting the size distribution of warhead fragments. *Mathematical Modelling*, 2(1), 19-32. https://doi.org/10.1016/0270-0255(81)90008-7

Department of Defense. Joint Chiefs of Staff. (6/1/1965- 10/31/1973). In J-3 (Operations) Directorate. Data Processing Division. ca. 1970-ca. 1975 (Ed.), Strategic air command combat activities report (SACCOACT) (Record Group 218: Records of the U.S. Joint Chiefs of Staff, 1941-1977 Trans.). (National Archives Identifier: 2385497 ed.). Series: Strategic Air Command Combat Activities Report (SACCOACT): US National Archive. Recovered from https://catalog.archives.gov/id/2367339 (accessed March 5, 2019).

Department of the Army Technical Manual (1966). Bombs and bomb components. (No. TM 9-1325-20 0). Washington, DC: Department of the Air Force Technical Order. Recovered from https://archive.org/details/TM91325200BombsAndBombComponents (accessed June 13, 2019).

ESRI (2019). ArcGIS ArcMap desktop: Release 10.6. Redlands, CA: Environmental Systems Research Institute. https://desktop.arcgis.com/en/arcmap/latest/tools/data-management-toolbox/project-raster.htm (accessed November 3, 2019).

ESRI (2020). ArcGIS pro desktop: Release 2.5. Redlands, CA: Environmental Systems Research Institute. https://pro.arcgis.com/en/pro-app/latest/tool-reference/data-management/clip.htm (accessed January 9, 2020).

Google Earth. (2023). Muang Souy, Xiangkhouang, Laos. 3D map, satellite image surface layer 19°30′34″ N, 103°02′55″ E. Retrieved from https://earth.google.com/web/ (accessed May 16, 2019).

Goto, D., Becker, R., Orzechowski, T., Springer, H., Sunwoo, A., and Syn, C. (2008). Investigation of the fracture and fragmentation of explosively driven rings and cylinders. *International Journal of Impact Engineering*, 35(12), 1547-1556. https://doi.org/10.1016/j.ijimpeng.2008.07.081

Ito, A. (2013). Global modeling study of potentially bioavailable iron input from shipboard aerosol sources to the ocean. *Global Biogeochemical Cycles*, 27(1), 1-10. https://doi.org/10.1029/2012GB004378

Jayasekera, D. and Kaluarachchi, J. (2015). Climate change impacts on water sustainability in the nam ngum river basin of laos. *WIT Transactions on Ecology and the Environment*, 196, 279-287. https://doi.org/10.2495/WRM150241

JICA and MOAF (2001). *Master Plan Study on Integrated Agricultural Development in Lao People's Democratic Republic*. Japan International Cooperation Agency (JICA) and Ministry of Agriculture and Forestry (MOAF).

Khamvongsa, C. and Russell, E. (2009). Legacies of war: Cluster bombs in Laos. *Critical Asian Studies*, 41(2), 281-306. https://doi.org/10.1080/14672710902809401

McCoy, A.W. (2002). A Companion to the Vietnam War. *America's Secret War in Laos, 1955-75*. Blackwell Publishing, pp 283-314. https://doi.org/10.1002/9780470997178.ch15

Open Development Initiative (2023). Open development laos; datahub. Retrieved from https://laos.opendevelopmentmekong.net/ (accessed April 22, 2019).

Pistocchi, A. (2014). *GIS based Chemical Fate Modeling: Principles and Applications*. John Wiley & Sons. https://doi.org/10.1002/9781118523667

Stronge, W.J., Ma, X.Q. and Zhao, L.T. (1989). Fragmentation of explosively expanded steel cylinders. *International Journal of Mechanical Sciences*, 31(11-12), 811-823. https://doi.org/10.1016/0020-7403(89)90026-X

Suter II, G.W. (2016). *Ecological Risk Assessment*. CRC press. https://doi.org/10.1201/9781420012569

Watmough, T. and O'shea, R.P. (1977). *Steel Alloy*. The United States of America as Represented by the Secretary of the Air Force, Patent US4043808A

WIIPA (2016). Costs of war: Human costs. https://watson.brown.edu/costsofwar/costs/human/civilians (accessed June 3, 2019)

Zannetti, P. (1986). *A new mixed segment-puff approach for dispersion modeling*. Atmospheric Environment (1967), 20(6), 1121-1130. https://doi.org/10.1016/0004-6981(86)90144-7